Measurement of Branching Ratios for the Dissociative Recombination of Cold HD$^+$ Using Fragment Imaging

D. Zajfman, Z. Amitay, and C. Broude

Department of Particle Physics, Weizmann Institute of Science, Rehovot 76100, Israel

P. Forck, B. Seidel, M. Grieser, D. Habs, D. Schwalm, and A. Wolf

Max-Planck-Institut für Kernphysik and Physikalisches Institut der Universität Heidelberg, D-69029 Heidelberg, Germany

(Received 21 April 1995)

Two-dimensional fragment imaging is used to determine branching ratios into final atomic states for dissociative recombination of vibrationally cold HD$^+$ molecules with electrons at variable energy. For low electron energies it is found that the dissociation proceeds via the $^1\Sigma_g^+$ state, leaving one of the fragments in the $n = 2$ level. At higher energies up to ≈ 20 eV, a pronounced angular anisotropy of the fragmentation is found on one of the previously measured resonances, allowing for conclusions about the symmetry of the dissociating states.

PACS numbers: 34.80.Gs

Interest in dissociative recombination (DR) arises out of the need to understand the basic properties of laboratory and astrophysical plasma, such as planetary ionosphere [1]. In this process, a free electron excites the ion and is simultaneously captured into a doubly excited molecular state. This state then dissociates along a repulsive potential curve, yielding fragments with translational energy and, possibly, internal excitation depending on the energy balance of the reaction. To date, mainly total cross sections for such processes have been measured, whereas only a few attempts were made to analyze the translational energy and the internal excitation of the fragments. However, this information is essential for a basic understanding of the DR process and for estimating its effect in a plasma environment; an example where the excited fragment states are important is the air glow occurring in the Earth's ionosphere, which is due to the recombination of O_2^+ through specific dissociative states [2].

The experimental problem to be solved in such studies is, in particular, the generation of ions in specific vibrational levels under conditions allowing for suitable measurements on the atomic products (e.g., in a well collimated fast ion beam). Earlier studies were able to analyze the production of D atoms in the $2p$ and the $n = 4$ excited states from the DR of D_2^+ using an optical detection method [3,4], but only for vibrationally hot ions with an unknown distribution over many vibrational states.

Recently, substantial progress in the production of vibrationally relaxed (cold) molecular ions was achieved by using the heavy-ion storage-ring technique [5], which enables one to store fast molecular ion beams for a time long enough to allow vibrational relaxation through spontaneous radiative decay. Measurements using this method on various vibrationally cold molecules such as HD$^+$, CD$^+$, and OH$^+$ have revealed new features in the DR cross section [6,7] at electron energies between 0 and ≈ 20 eV.

In the present experiment, we have combined the storage-ring technique and a two-dimensional fragment imaging method to measure the kinetic energy released in the DR of cold HD$^+$ molecules. Since the initial molecular state and the electron energy are well defined, the internal excitation energy of the atomic products can be inferred using energy conservation. The HD$^+$ molecule, for which the DR process can be depicted as

$$\text{HD}^+ + e \rightarrow \text{HD}^{**} \rightarrow \text{H}(nl) + \text{D}(n'l'), \qquad (1)$$

with HD** denoting the doubly excited dissociating state, is the simplest molecular ion that can be efficiently cooled internally in a storage ring [8]. It is important as a test case for the understanding of this method because calculations are available for the relevant excited state potential curves, which are similar to those of H_2 [9] under the Born-Oppenheimer approximation (see Fig. 1). Previous experiments with HD$^+$ and H_2^+ have shown that the DR cross section at low energy is $\approx 3 \times 10^{-16}$ cm^2 at an energy of $E = 0.1$ eV [10] and decreases as E^{-1} up to ≈ 1 eV [6]. At energies of ≈ 9 and ≈ 16 eV, two broad resonances appear that have been explained by the formation of HD** states with the $(2p\sigma_u)\,^2\Sigma_u^+$ and $(2p\pi_u)\,^2\Pi_u$ states of HD$^+$ as the predominant core orbitals [6] (see Fig. 1). Retaining the notation of previous authors [9], we label these doubly excited states by Q_1 and Q_2, respectively.

The experiment was carried out at the Test Storage Ring (TSR) [5] located at the Max-Planck-Institut für Kernphysik, Heidelberg. The experimental setup has been described previously [6] and will be presented here only shortly. A beam of 2.08-MeV HD$^+$ ions was produced by a Van de Graaff accelerator with a standard Penning ion source and injected into the TSR. Typically 10^7 particles circulated in the ring with a lifetime of ≈ 18 s. The circulating ion beam was merged with the 5-cm-diam, quasimonochromatic electron beam of the electron cooler over a length of 1.5 m, providing electrons at a typical density of 2×10^6 cm^{-3} and a temperature of ≈ 0.015 eV in the comoving reference frame. Electron cooling was
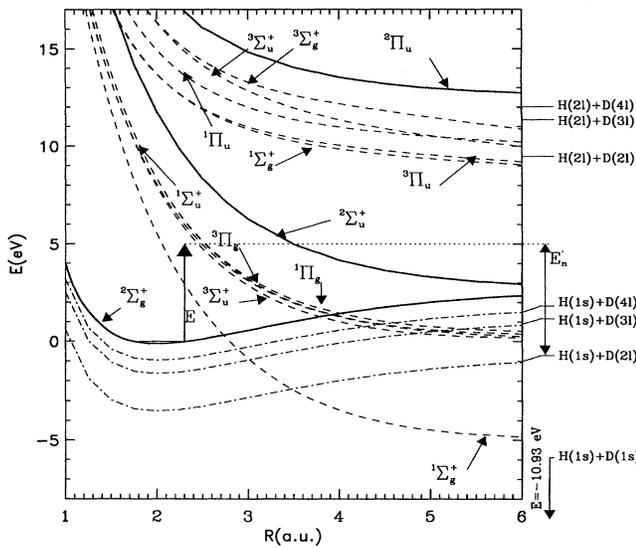
FIG. 1. Relevant potential curves for HD$^+$ (thick solid lines) and HD (dashed and dash-dotted lines), showing the ground state and the two excited states of HD$^+$, the lowest singly excited Rydberg states of HD (dash-dotted) and the lowest doubly excited states of HD (dashed) below the $^2\Sigma_u^+$ and $^2\Pi_u$ states of HD$^+$. A more complete set of potential energy curves can be found in Ref. [9]. The asymptotic energies for various final states of the fragments (D can be replaced by H and vice versa) are drawn on the right-hand side of the picture. The relation between the energy release E_n' and the electron energy E is illustrated.

applied for about 3 s before the measurement in order to ensure equal velocity of ions and electrons, to reduce the diameter of the ion beam to about 2 mm, and to allow vibrational cooling of the HD$^+$ molecules [8].

An 80-mm-diam Chevron microchannel-plate (MCP) detector was mounted straight ahead of the cooler section at a distance of 6 m to detect the neutralized particles from the cooler region as well as from remanent gas collisions. Each impact on the MCP produced a light spot on a phosphor screen located 1 mm behind the MCP. The image generated by these spots was digitized using a charge coupled device (CCD) camera, coupled to a fast frame grabber device [11]. On analysis, the positions of the light spots were determined using a straightforward peak finding procedure, and the relative projected distance between any two fragments on the plane of the detector was deduced. The detector was operated in a trigger mode in order to suppress random coincidences between single hits due to two unrelated single fragments produced by collisions with the residual gas (such as HD$^+$ + X → H$^+$ + D + X or D$^+$ + H + X, where X denotes a residual gas molecule). In this mode the phosphor screen is switched off in about 20 μs whenever an impact on the MCP is detected by a fast photomultiplier, located close to the CCD camera. Since the maximum difference

in arrival times for two fragments of a DR event is about 1 ns, while the average interval between two single events depends on the neutral rate, kept below 10^3 s^{-1}, the random coincidence rate is strongly suppressed; data were taken at a rate of 25 frames per second with a true-to-random coincidence ratio of >100. The position resolution of the detector was ≈100 μm.

For a DR event at a distance s from the detector, with an initial angle θ of the internuclear axis of the molecule relative to the beam direction, and with a final excitation state n the projected transverse distance D of the two neutral fragments is given by $D = s \delta_n \sin\theta$, where

$$\delta_n = (E_n'/E_b)^{1/2}(m_H + m_D)/(m_H m_D)^{1/2} \qquad (2)$$

is the maximum angle between the fragments, occurring for $\theta = \pm\pi/2$ and determined by the energy release E_n' in the center-of-mass (c.m.) frame, the beam energy $E_b = 2.082(1)$ MeV, and the fragment masses m_H, m_D. For a given c.m. electron energy E, the energy release $E_n' = E - E_n$ reflects the internal energy E_n of the fragments, i.e., the asymptotic energy level of the separated atoms relative to the initial energy level of the molecular ion (see Fig. 1).

The observed spectrum of projected distances $P(D)$ is represented by an average over the longitudinal extension of the interaction region (at a distance from the detector ranging from $s_1 = 5.72$ m to $s_2 = 7.21$ m, as given by the beam geometry), over the molecular orientation θ, and over the final states n. In particular, an isotropic distribution of fragments in the c.m. frame, i.e., a DR cross section independent of the initial molecular orientation, for a single final state n yields [12]

$$P_n(D) = (\arccos x_2 - \arccos x_1)/L\delta_n, \qquad (3)$$

with $x_{1,2} = \min(1, D/s_{1,2}\delta_n)$. This spectrum rises from 0 at $D = 0$ to a maximum at $D = s_1\delta_n$ and then drops to 0 at $D = s_2\delta_n$. The information on the energy release is mainly contained in the drop at high D, whose relative sharpness is determined by the ratio of the interaction length $L = s_2 - s_1$ to the average distance from the detector. The total spectrum is given by $P(D) = \sum_n b_n P_n(D)$ with the (normalized) coefficients b_n representing the branching ratios.

Figure 2(a) shows the measured projected-distance spectrum at $E = 0$. At this energy, the only asymptotic states which are energetically accessible for HD$^+$ ions in their vibrational ground state are those for which at least one atom is in the ground state and the other one is in either the $n = 1$ state [H(1s) + D(1s)] or the $n = 2$ state [H(1s) + D(2s) or D(1s) + H(2s)]. Theory predicts that at this energy DR occurs through the lowest lying $^1\Sigma_g^+$ state. This curve crosses the singly excited HD Rydberg states at internuclear distances of 2.5–3.5 a.u. (see Fig. 1) but does not connect to the $n = 1$ dissociation limit. Thus, if $^1\Sigma_g^+$ is the dominant dissociating state, only the $n = 2$ asymptotic states should be
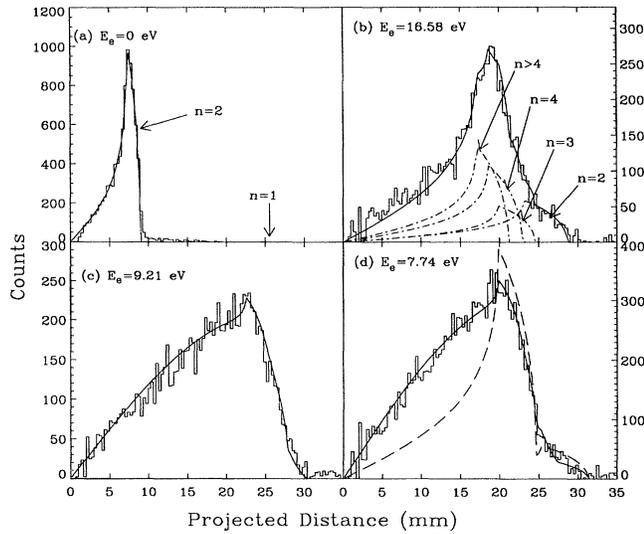
FIG. 2. Distribution of relative distances between the fragments at the detector for various settings of the average c.m. electron energy E of (a) 0, (b) 16.58 eV, (c) 9.21 eV, and (d) 7.74 eV; the background has been subtracted. The calibration of the D scale in mm is known within $\pm 10\%$. Smooth lines are fits of theoretical distributions $P(D)$, where the amplitudes of the different contributions were varied and the parameters $s_1 = 5.72$ m and $s_2 = 7.21$ m were fitted by signal (a). The dash-dotted lines in (b) indicate various components for different final atomic states, and the dashed line in (d) represents the best fit based on an isotropic distribution, as opposed to the anisotropic fit shown by the full line.

formed. Our results are in perfect agreement with this theoretical prediction, as shown in Fig. 2(a) by the solid line which was calculated for isotropic fragmentation and an energy release of $E_2' = 0.726$ eV; the arrow indicates the expected maximal projected distance of DR events involving the $n = 1$ asymptotic state (energy release $E_1' = 10.93$ eV), where in fact no events above the noise level could be observed. Moreover, this shows that no significant vibrational excitations are present in the stored beam: The additional energy release of 0.288 eV from the first vibrational level would be easily resolvable in the projected-distance spectrum.

Figure 2(b) shows the projected-distance spectrum at $E = 16.58$ eV, obtained after adjusting the electron beam energy accordingly. At this energy a prominent resonance appears in the DR cross section [6], ascribed to dissociation through the Q_2 states. For this path, one atom is produced in a $2s$ or $2p$ state and the other one in higher excited states with $n \geq 2$ (see Fig. 1). We have fitted our data with the sum of spectra for energy releases E_n' corresponding to the different asymptotic states n [full line in Fig. 2(b)]. The relative amplitudes b_n of these contributions (dash-dotted lines) yield the branching ratios of $(20 \pm 1)\%$ for $n = 2$, $(12 \pm 3)\%$ for $n = 3$, $(33 \pm 3)\%$ for $n = 4$, and $(35 \pm 5)\%$ for $n \geq 5$. The

contributions for $n \geq 5$ appear as a single component as the energy difference between consecutive states becomes unobservable. In particular, the contribution of the $n = 2$ state is clearly visible as a shoulder on the right side of the spectrum.

In Figs. 2(c) and 2(d) we have plotted the projected distance between the two fragments at $E = 9.21$ eV and at $E = 7.74$ eV. These energies lie close to the lower peak in the DR cross section [6], attributed to dissociation through the doubly excited Q_1 states. The final states are of the type $H(1s) + D(nl)$ or $D(1s) + H(nl)$. On dissociation along the Q_1 states, many anticrossings with Rydberg levels are encountered, which determine the final state distribution depending upon the details of the anticrossings and the dynamics.

One can immediately see that the line shape in this case is very different from the two previous cases, and that many more molecules dissociate with a small relative projected distance. Attempts to fit the data with a superposition of states for isotropic fragmentation were unsuccessful, as demonstrated by the result of one such fit displayed as a dashed curve in Fig. 2(d). However, since the distances mainly represent the *transverse* momentum after fragmentation, they are sensitive to anisotropies in the distribution of fragmentation angles θ. As discussed by Dunn [13] already more than 30 years ago, the DR rate can in fact depend on the orientation of the molecular axis relative to the incident electron direction, since the doubly excited state must have the same symmetry as the complete electronic wave function prior to the collision. Anisotropies in the angular distribution of molecular fragments were already observed in the case of electron impact dissociation [13,14].

For dissociative recombination involving doubly excited Σ and Π states, the angular distributions are expected [15] to be represented by a sum of $\cos^2\theta$ or $\sin^2\theta$ terms, for which projected fragmentation spectra $P_{n,c}(D)$ and $P_{n,s}(D)$, respectively, can be calculated similar to the isotropic case discussed above. Thus we can represent $P_n(D)$ as a sum of these two normalized contributions, $P_n(D) = (1 - a_n)P_{n,s}(D) + a_nP_{n,c}(D)$, and then sum over n as before; isotropic distributions [Eq. (3)] are regained for $a_n = 1/3$. Fitting the data by these spectra, shown as full lines in Figs. 2(c) and 2(d), now yields excellent agreement. For $E = 9.21$ eV, the branching ratios following from the coefficients b_n are $<1\%$ for $n = 2$, $(72 \pm 8)\%$ for $n = 3$, and $(28 \pm 7)\%$ for $n \geq 4$. A very strong angular anisotropy of character $\cos^2\theta$ with $a_3 = 0.9 \pm 0.1$ is found for the final states $H(1s) + D(3l)$ or $D(1s) + H(3l)$, while the $n \geq 4$ contributions appear to be mainly isotropic. At $E = 7.74$ eV, the branching ratios are $(8 \pm 1)\%$ for $n = 2$, $(70 \pm 10)\%$ for $n = 3$, and $(22 \pm 7)\%$ for $n \geq 4$, again with $a_3 = 0.9 \pm 0.1$ and nearly isotropic angular distribution for the $n = 2$ and $n \geq 4$ channels. It is interesting to point out that our observed branching ratios are in qualitative agreement with

an earlier optical measurement for the $n = 2$ and $n = 4$ states of vibrationally hot D_2^+ ions [3,4], where it was found that these two states account for only a small fraction of the total cross section. The present results are also in qualitative agreement with the theoretical calculations of Zhdanov and Chibisov [16] which predicted that $n = 3$ is the dominant final state at these energies.

The measurement of the anisotropy makes it possible to identify the symmetry of the states responsible for the lower peak of the DR cross section at ≈ 8.6 eV, in particular, for the $n = 3$ channel found to be largely dominant. Four potential curves with symmetries $^{1,3}\Sigma_u^+$ and $^{1,3}\Pi_g$ are consistent with the observed branching ratios as they cross the $n = 3$ level at ≈ 5 a.u., but not the $n = 2$ level (see Fig. 1). Considering the $^2\Sigma_g^+$ symmetry of the HD^+ ground state and the angular behavior of the DR cross section as tabulated by Dunn [13], the observed $\cos^2\theta$ distribution (corresponding to the "O|X" case of Table I, line 1 in Ref. [13]) clearly indicates that the dissociation to $n = 3$ is mostly due to doubly excited states with a Σ_u^+ symmetry, the most likely being the $^3\Sigma_u^+$ state due to its statistical weight [9]. On the other hand, the mostly isotropic $n = 2$ contribution starting to appear at lower energy ($E = 7.74$ eV) should be due to a doubly excited state with Σ_g^+ symmetry ("X|X" in Ref. [13]); in fact, the lowest $^1\Sigma_g^+$ state shown in Fig. 1 is the only dissociative state to cross the $n = 2$ Rydberg state.

Similarly, for the higher peak in the DR cross section ($E = 16.58$ eV), the fact that the projected-distance histogram is well fitted using an isotropic angular distribution indicates that none of the symmetries Σ_u^+ or Π_u (see Fig. 1) alone can be dominant in the DR process, as they would yield an anisotropic distribution; there are either contributions of similar size from both these symmetries or possibly contributions with Σ_g^+ symmetry alone, which would be isotropic.

To conclude, we have measured for the first time branching ratios to final atomic states after DR of vibrationally cold diatomic molecules by means of two-dimensional imaging of the fragments. Combining vibrational cooling in a heavy-ion storage ring and fragment imaging with the merged-beam technique we could identify contributions to the DR cross section for specific initial *and* final states, thus providing a handle on one of the most serious problems in comparing experimental DR data with theoretical calculations. The branching ratios and state symmetries inferred from the projected-distance spectra allow conclusions on the most important doubly excited states along which the molecule dissociates. For a more complete theoretical understanding, clearly not only the capture process at short internuclear distances (≤ 6 a.u.) but also the full reaction path up to large distances has to be considered. In contrast to the earlier optical technique, the method employed here can be applied to any type of molecule. It is planned to further develop the imaging detector in order to measure also the relative fragment arrival times, and to use a shorter interaction length between electron and ion beam in order to increase the resolution for the energy release E_n'.

[1] J. N. Bardsley and M. A. Biondi, Adv. Mol. Phys. **6**, 1 (1970).

[2] J. L. Fox, in *Dissociative Recombination: Theory, Experiment and Applications*, edited by B. R. Rowe, J. B. A. Mitchell, and A. Canosa (Plenum Press, New York and London, 1993), p. 219.

[3] R. A. Phaneuf, D. H. Crandall, and G. H. Dunn, Phys. Rev. A **11**, 528 (1975).

[4] M. Vogler and G. H. Dunn, Phys. Rev. A **11**, 1983 (1975).

[5] D. Habs *et al.*, Nucl. Instrum. Methods Phys. Res., Sect. B **43**, 390 (1989).

[6] P. Forck *et al.*, Phys. Rev. Lett. **70**, 426 (1993).

[7] P. Forck *et al.*, Phys. Rev. Lett. **72**, 2002 (1994).

[8] Z. Amitay, D. Zajfman, and P. Forck, Phys. Rev. A **50**, 2304 (1994).

[9] S. L. Guberman, J. Chem. Phys. **78**, 1404 (1983).

[10] H. Hus *et al.*, Phys. Rev. Lett. **60**, 1006 (1988).

[11] D. Kella *et al.*, Nucl. Instrum. Methods Phys. Res., Sect. A **329**, 440 (1993).

[12] Z. Amitay, D. Zajfman, and P. Forck (to be published).

[13] G. H. Dunn, Phys. Rev. Lett. **8**, 62 (1962).

[14] R. J. van Brunt and L. J. Kieffer, Phys. Rev. A **2**, 1293 (1970).

[15] T. F. O'Malley and H. S. Taylor, Phys. Rev. **176**, 207 (1968).

[16] V. P. Zhdanov and M. I. Chibisov, Sov. Phys. JETP **47**, 38 (1978).